Growth mode transfer of self-assembled CdSe quantum dots grown by molecular beam epitaxy

Y.J. Lai[a], Y.C. Lin[a], C.P. Fu[a], C.S. Yang[a], C.H. Chia[a], D.S. Chuu[a], W.K. Chen[a], M.C. Lee[a], W.C. Chou[a,*], M.C. Kuo[b], J.S. Wang[b]

[a]Department of Electrophysics, National Chiao Tung University, Hsin-Chu, Taiwan 30010, ROC
[b]Department of Physics, Chung Yuan Christian University, Chung-Li 32023, Taiwan

Abstract

Self-assembled CdSe/ZnSe quantum dots (QDs) were grown at various growth temperatures on GaAs (0 0 1) by molecular beam epitaxy. An optimum growth temperature for CdSe/ZnSe QDs was found to be 260 °C. The Stranski–Krastanow (SK) growth mode was confirmed clearly by atomic force microscopy images. The coherent SK QDs were observed from 2.5 monolayers (MLs). Two types of QDs were found with the CdSe coverage of 3.0 MLs. It was attributed to a growth mode change from the coherent SK growth mode to the ripening growth mode. A schematic diagram of the growth mechanism of self-assembled CdSe QDs was presented. Moreover, the photoluminescence spectra of samples with various thicknesses were investigated. A dramatic change of optical properties confirmed that the QD structure formed with thickness above 2.5 MLs. Finally, the dot size and the density distributions were controlled after growth by in-chamber thermal annealing. For the sample grown at 3.0 MLs, the distribution of dot sizes was controlled from 6.0 to $6.5 \times 10^3 \, \text{nm}^3$ at an annealing temperature of 400 °C.
© 2005 Published by Elsevier B.V.

1. Introduction

The growth of quantum dot (QD) structures (or semiconductor nano-structures) for opto-electronic devices have gained considerable attention in recent years, because the QD laser can achieve low threshold current density, high gain and high quantum efficiency [1–3]. In III–V compound semiconductor systems, laser diode devices with InAs/GaAs QD structures were successfully demonstrated [4]. Successful examples were also found in the II–VI compound semiconductor-based QD structures, such as laser diodes and bright light-emitting diodes [5,6]. CdSe QDs grown on the ZnSe buffer layer constitute one of the most well-studied systems among the II–VI compound semiconductors. The lattice constant of ZnSe is almost matched to that of the GaAs substrate and the lattice constant of CdSe is mismatched by about 7.2% to that of ZnSe buffer layer [7]. Therefore, the CdSe/ZnSe QD system is similar to the InAs/GaAs system, which also exhibits a lattice mismatch of approximately 7.1% between the InAs QD and the GaAs buffer [8]. The lattice mismatch between InAs and GaAs generates for just enough strain energy to form the QD structures with a wetting layer of about 2.0 monolayers (MLs) under the Stranski–Krastanow (SK) growth mode [9]. However, the 2D (two-dimensional) to 3D (three-dimensional) growth of dots in CdSe/ZnSe system is not simple like a well-defined 2D wetting layer (layer-by-layer) or Frank van der Merve (FM) mode transferring to SK 3D growth. The Cd concentration in the

*Corresponding author. Tel.: +11 886 3 5712121 56129.
E-mail address: wuchingchou@mail.nctu.edu.tw (W.C. Chou).

initial CdSe deposited on ZnSe buffer layer is not uniform. The Cd-rich regions can be regarded as 2D-like islands (or 2D platelets) that act as precursors for the formation of coherent 3D islands [10]. A great deal of effort has been devoted to study the fundamental properties [11–15] of the CdSe/ZnSe QD structures as well as the potential applications of incorporating QD structures in laser diodes for emission in the green and blue wavelength range [6].

In 1996, Xin et al. [16] studied the morphology of the CdSe QDs using atomic force microscopy (AFM). Changes in the dot size and the density with time at room temperature were observed. After 2 years, Lee et al. [17,18] proposed that this behavior of the change in dot size and density with time be regarded as ripening. A systematic investigation of ripening of CdSe self-assembled QDs on ZnSe was reported. They investigated the size and density of the QDs as functions of time after the termination of the deposition of CdSe. The dynamics of the ripening process are interpreted in terms of the theory of Ostwald ripening. Moreover, Daruka and Barabasi [19] theoretically defined an equilibrium phase diagram for the QD growth mode. Their theory, described the transformation of the growth mode of QD as a function of the coverage and the lattice mismatch between QD and buffer. They also concluded that the free energy of the ripened dot decreases monotonically with the increases in dot size; accordingly, a tendency exists to accumulate all available material in an island as large as possible. As a result, some dots grow with time at the cost of other dots. This result was consistent with the observation of Lee et al. [17]. In this work, as the coverage increased, a transfer of the QD growth mode from the SK mode to the ripened mode was observed in an AFM study. The observations herein are consistent with the theoretically prediction in Ref. [19].

Applications of QD structures in opto-electronic devices inevitably encounter the problems of size fluctuation. A size fluctuation can broaden the emission spectrum and reduce the emission intensity at the designed wavelength [20]. Artificially controlling the size distribution during the growth of QDs is crucial to reduce the size fluctuation and varying the emission wavelength. Thus good artificial control is the solution to improve the fabrication of opto-electronic devices with QDs. In current study, the effects of the substrate temperature and the post-growth annealing temperature on the size-distribution of QDs were also studied to explore the possible means of controlling the size.

2. Experimental procedure

Self-assembled CdSe QDs were grown on a ZnSe buffer layer using Veeco Applied EPI 620 MBE system. The ZnSe buffer layer was grown on the epi-ready GaAs substrate. Before growth, the GaAs surface was cleaned by chemical etching with $H_2O:NH_4OH:H_2O_2$ in the ratio 50:5:5 for 2 min, followed by rinsing with D.I. water and final drying with nitrogen gas. The time between chemical etching and the transfer of the substrate into the vacuum chamber was less than 5 min. The residual oxide on the GaAs surface was desorbed by the substrate temperature (T_G) of 650 °C. Desorption process was monitored by a reflection high-energy electron diffraction (RHEED) pattern. After desorption, T_G was decreased to 350 °C to grow the ZnSe buffer layer. The ZnSe buffer layer includes several MLs grown by migration enhance epitaxy (MEE) [21], and a thickness of 20 nm grown by the conventional MBE growth mode. The average roughness of the ZnSe buffer layer is about 0.28 nm. After the flat ZnSe buffer layer was deposited, the growth of the self-assembled CdSe QDs began. Table 1 presents the sample parameters in the AFM and photoluminescence (PL) study. Samples 1, 2 and 3 have the same average coverage of CdSe (3.0 MLs), but the values of T_G were 240, 260 and 280 °C, respectively. The T_G values of samples 4–9 were fixed at 260 °C. The average coverage of CdSe for samples 4–9 were between 2.0 and 3.7 MLs. In order to compare the surface roughness of ZnSe buffer layer and other samples, a sample was grown ZnSe only. The average coverage of CdSe was determined by the growth duration and the growth rate, which was calibrated by a thick CdSe epilayer whose growth conditions were the same as those of QDs. The growth rate was determined by measuring the growth duration and the thickness of the thick CdSe epilayer. The thickness was estimated from the energy spacing of the interference peaks of the reflectivity spectrum. The thickness of the CdSe layer was further verified by optical microscopy with a resolution of 0.1 μm. For a CdSe epilayer with a thickness of 1 μm and accuracy of 0.1 μm, the uncertainty of the growth rate is about 10%. It implies the accuracy of the CdSe coverage is about 10%, i.e. the uncertainty is less than several tenths of MLs for the CdSe coverage of 2.0–3.7 MLs. The above information is crucial for determining the thickness of the wetting layer. The thickness of the ZnSe buffer layers for samples 1–9 was 20 nm while that of the ZnSe for samples 10 and 11 was 50 nm. Above the ZnSe buffer layer, CdSe

Table 1
Sample parameters

Sample	1	2	3	4	5	6	7	8	9	10	11
Buffer (nm)	20	20	20	20	20	20	20	20	20	50	50
CdSe (MLs)	3.0	3.0	3.0	2.0	2.5	2.7	3.3	3.5	3.7	3.0	3.0
T_G (°C)	240	260	280	260	260	260	260	260	260	260	260
T_A (°C)	—	—	—	—	—	—	—	—	—	—	400

was grown with an average coverage fixed at 3.0 MLs. In-chamber thermal annealing process was performed for sample 11. An annealing temperature (T_A) of 400 °C was chosen. Buried dots were also prepared for optical studies. The growth condition of the samples for the optical study was the same as that of samples 4–9, before a 20 nm capping layer of ZnSe was deposited.

The NT-MDT SOLVER P47 AFM was employed to study the morphology. The measurement was carried out using the semi-contact mode. The scan steps in the x and y directions were both 4.8 nm. The resolution was 0.01 nm in the z direction. The silicon tip was conic. Its diameter (D) and height (H) were 30 and 70 nm, respectively (the aspect ratio, $\alpha = H/D = 7/3$). The aspect ratio of silicon tip is much larger than that of the CdSe QD grown in current study. The 351.0 nm line from an argon

ion laser was used to excite the PL spectra. A SPEX 1403 spectrometer, equipped with a thermoelectric cooled photomultiplier tube, was used to measure the temperature dependence of the PL spectra. Typically, the slit widths were set to 200 μm to yield a spectral resolution of better than 0.2 meV.

3. Results and discussion

Figs. 1(a)/(b), (c)/(d) and (e)/(f) show the plane view/3D view of AFM for sample 1 ($T_G = 240$ °C), sample 2 ($T_G = 260$ °C) and sample 3 ($T_G = 280$ °C), respectively. The vertical axis labeled with black and white contrast was drawn at the right-hand side of the plane views to represent the height of a QD. In Figs. 1(a) and (b), large islands were observed. The dots are large and their sizes
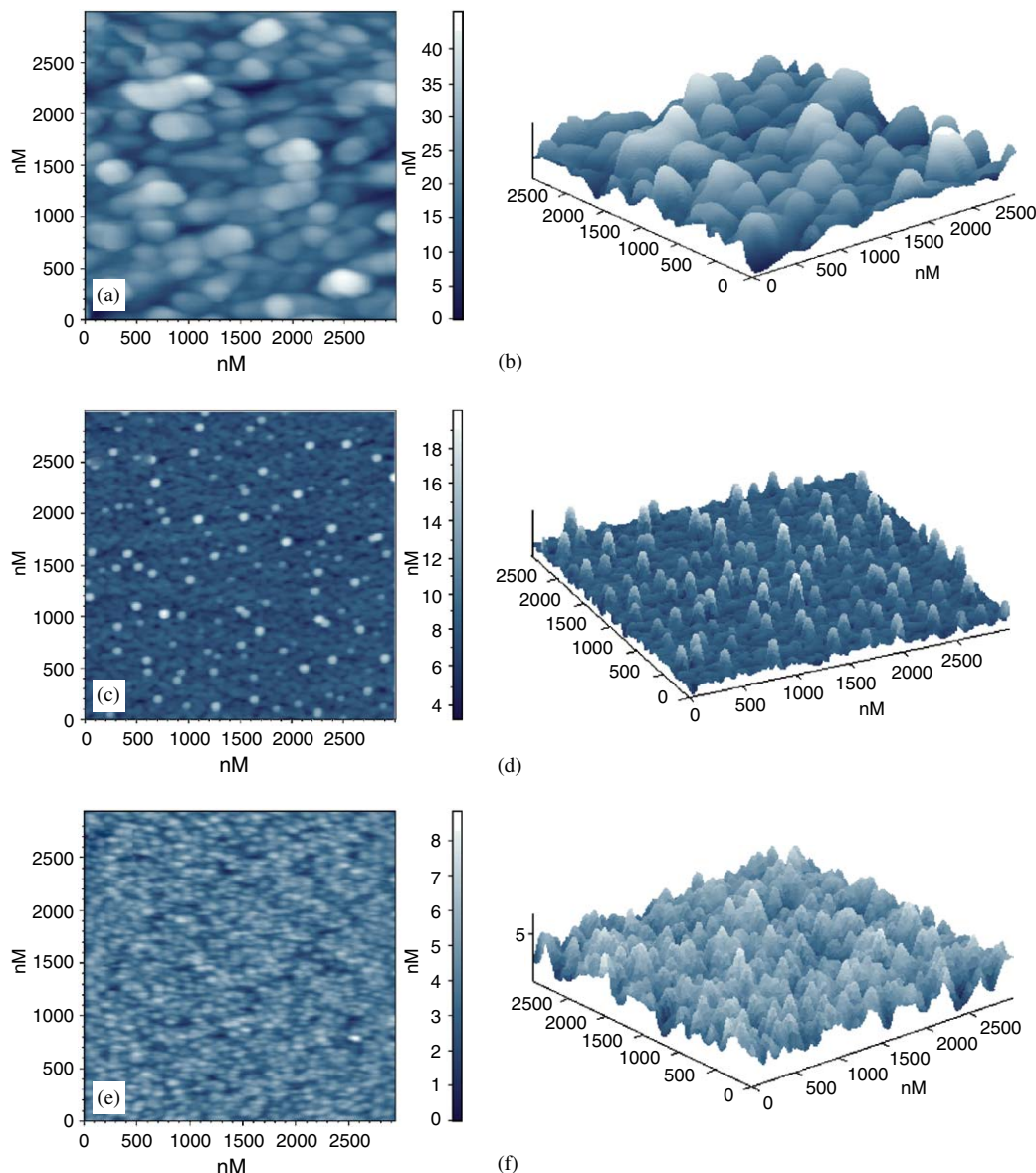
Fig. 1. AFM plane view and three-dimensional view for samples 1 ($T_G = 240$ °C), 2 ($T_G = 260$ °C) and 3 ($T_G = 280$ °C).

are not uniform. As T_G increased slightly for sample 2, self-assembled CdSe QDs form, as depicted in Figs. 1(c) and (d). The QDs were divided into a group of large dots ($H > 4$ nm) and small dots ($H < 4$ nm). The average diameter of the larger (smaller) dots is approximately 86 (66) nm and the mean height is 5.35 (2.21) nm. The dot density of both groups is approximately 2.0×10^9 cm^{-2}. The dot density increased abruptly as T_G increased further for sample 3, as shown in Figs. 1(e) and (f). The dots were very close to each other. As a result, some dots were connected. Random dot shapes were observed. Also, the size distribution was very broad. This sample is less useful for further study. The above result reveals that T_G is an important parameter for growth of QDs. T_G must not be too low to ensure that sufficient kinetic energy is provided for the migration of the CdSe molecules. However, if T_G is too high, the nucleation of the properly sized CdSe QDs becomes difficult. In summary, a T_G of 260 °C is the most suitable for further morphology study.

A systematic investigation of CdSe QDs for various coverages was done. Fig. 2 shows the plane view of AFM for samples 2, 4–9, and ZnSe buffer layer. At both ends of the axis, the black and white represent the lowest point at 0 nm and the highest point at 16 nm. In Fig. 2(a), the weak black and white contrast indicates the smooth surface of the ZnSe buffer layer. The average roughness of the ZnSe surface is less than 0.28 nm. When 2.0 MLs CdSe was deposited (sample 4) on ZnSe buffer layer, the average surface roughness changed from 0.28–0.42 nm. No clear 3D island formation was observed in Fig. 2(b). When the average coverage was further increased to 2.5 MLs (sample 5), the QD structure still could not be observed but the surface roughness increased slightly to 0.45 nm. However, there were many small spots on the sample surface observed in Figs. 2(b) and (c). The average aspect ratio, $\alpha = H/D$, of these small spots were 10^{-3}, which is much less than 3D QD structure. Therefore, they could be considered to the 2D-like islands. Similar result reported by

Strassburg et al. [22] the density of the 2D-like islands is almost invariant with respect to the CdSe coverage. The formation of this island-type starts already when the first monolayer is deposited. The 2D-like islands cannot be correlated with a SK process. As the average coverage increased further to 2.7 MLs (sample 6), as shown in Fig. 2(d), the 3D dots began to appear. The dot density of sample 6 was 2.0×10^8 cm^{-2}. The average dot height and diameter were 2.95 and 68.3 nm, respectively. The average aspect ratio was 4.3×10^{-2}, which is much smaller than that ($\alpha = 0.25$) measured using the amplitude scan of the taping mode [16]. However, the above observation indicates that the critical thickness is between 2.5 and 2.7 MLs for the transition of 2D to 3D growth, i.e. the thickness of the wetting layer is about 2.5–2.7 MLs.

In Fig. 2(e), the average coverage was 3.0 MLs (sample 2) and two groups of QD were observed. The average diameter and height of the larger (smaller) dots were 86 (66) and 5.35 (2.21) nm, respectively. The dot density of the larger (smaller) dots was 15.2×10^8 (4.8×10^8) cm^{-2}. The coexistence of small and large dots in Fig. 2(e) was similar to that in the second ripen (R_2) growth mode, which was theoretically defined by Daruka and Barabasi [19,23], as shown in the equilibrium phase diagram of Fig. 3. Fig. 3 refers to phase diagram II in Ref. [23]. It was obtained by minimizing the sum of the energy of the strained overlayer, the free energy of the QDs and the total energy density of the ripened islands. The x-axis represents the misfit between the buffer layer and the material grown above. While the y-axis represents the average coverage of QD. For a very small misfit and low coverage, only the 2D growth mode, i.e. the FM mode, is allowed. For a misfit that is less than but close to 0.063, the growth mode starts with the FM mode. If the average coverage is above 3.0 MLs, a ripened (R_1) growth mode begins. For misfit between 0.068 and 0.075, the growth starts with the FM mode and proceeds to the SK_1 mode and then to the R_2 mode as the coverage increases. In the SK_1 growth mode,
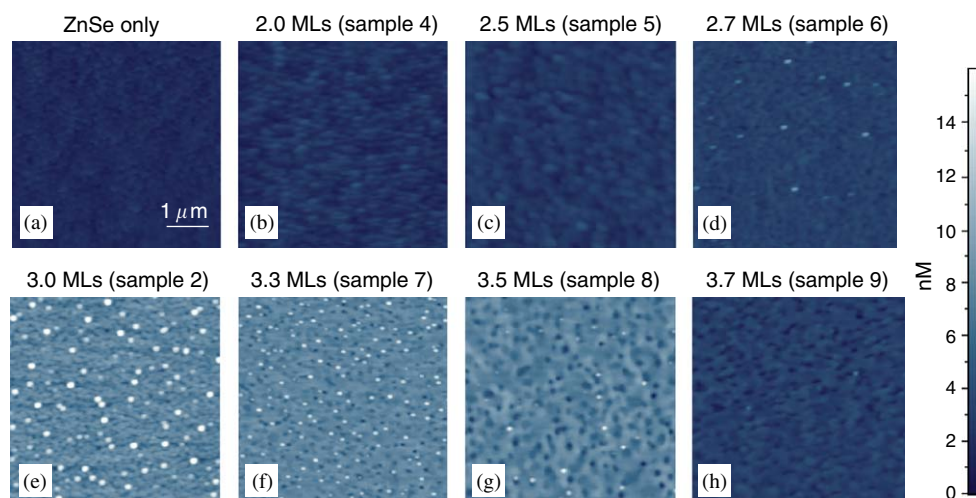

Fig. 2. AFM plane view for samples with the CdSe coverage of (a) 0, (b) 2.0, (c) 2.5, (d) 2.7, (e) 3.0, (f) 3.3, (g) 3.5 and (h) 3.7 MLs, respectively.
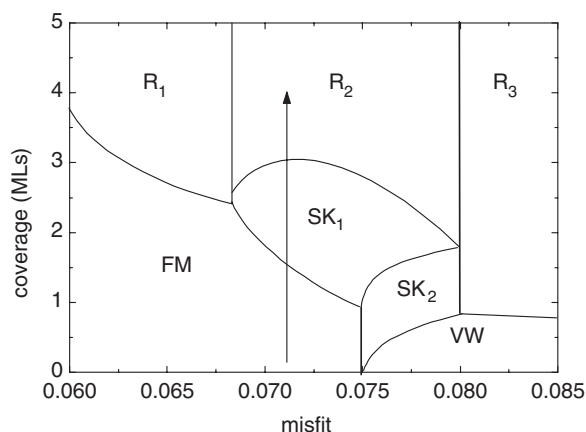
Fig. 3. Equilibrium phase diagram of the self-assembled QDs, obtained from reference 19 and 23 by minimizing the sum of the energy of the strained overlayer, the free energy of the QDs and the total energy density of the ripened islands. The x-axis is the misfit between the buffer layer and the material grown above. The y-axis represents the average coverage of QD.
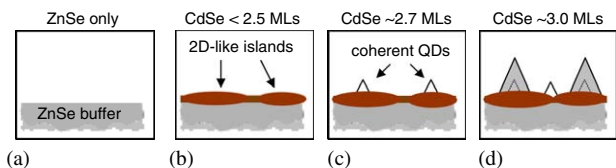

Fig. 4. Schematic diagram of the growth dynamics for the self-assembled CdSe QDs: (a) ZnSe only, (b) CdSe coverage is smaller than 2.5 MLs, (c) CdSe coverage is about 2.7 MLs, and (d) CdSe coverage is about 3.0 MLs.
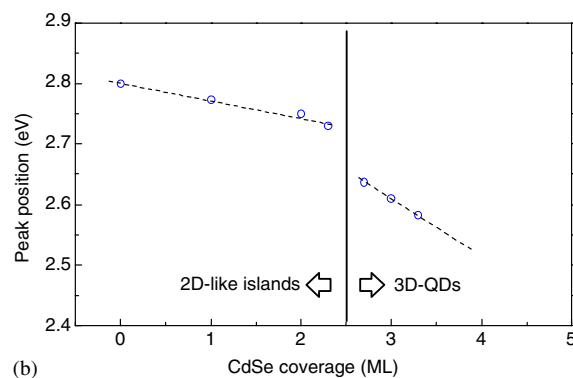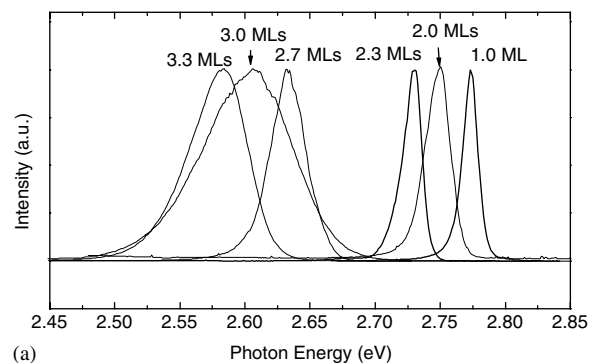

Fig. 5. (a) PL spectra from the CdSe QDs for various coverages. The CdSe coverage increases from 1.0–3.3 MLs. (b) PL peak position versus CdSe coverage. Two slopes are observed.

the 3D QDs were grown on the wetting layer. In the R_2 growth mode, the *larger ripened QDs* and the *smaller SK QDs* coexist. In current study, the misfit between the ZnSe buffer layer and the CdSe QD is about 0.071, a possible transfer of the QD growth mode indicated by the solid line in Fig. 3. The equilibrium phases of the Volmer–Weber (VW), SK_2 and R_3 growth modes are not discussed herein, since in this work, the misfit is less than 0.1.

To summarize the above discussions, a schematic growth dynamics was shown in Fig. 4. Figs. 4(a)–(c), which correspond to CdSe coverages of 0, 2.5 and 2.7 MLs, respectively, show the SK growth mode of CdSe QDs. Note that the formation of 2D-like island starts already when the first monolayer is deposited. The 2D-like islands cannot be correlated with a SK process [22]. In Fig. 4(d), the CdSe coverage was 3.0 MLs; the original smaller QDs grow into larger ripened QDs, while some smaller SK dots appeared in the flat spaces to relax the remaining stress. As a result, the growth mode changed from the SK mode to the R_2 growth mode. Moreover, investigation of the dot size changed with time was done. The significant increase in the size of the ripened dots with time at room temperature was observed, while the size of the SK dots (smaller dots) did not clearly change with time. The dynamics of the ripening process are interpreted in terms of the theory of Ostwald ripening. When CdSe coverage increases to

3.3 MLs, the significant uniform dot size distribution was observed. This result implies that there may exist a critical size for the ripened dot. The dot size would be able to increase upto the critical size. The larger QDs would be broken, when dot size increased over the critical size. At the same time, the substrate temperature provides the kinetic energy for the materials to migrate. The materials which originate from the broken larger dots would form these uniform dots. (The ripening process still works even at room temperature. Therefore, the higher substrate temperature could be able to enhance the migration process.) For the CdSe coverage of over 3.5 MLs, as shown in Figs. 2(g) and (h), a transformation from 3D to defected 2D growth was observed. In this case, a coherently self-assembled QD formation was impossible. This result is consistent with that observed by Schikora et al. [24], who showed that the CdSe stacking faults appear at the coverage of approximately 3.1 MLs, according to cross-sectional TEM. In summary, a coherent SK growth mode was observed at $T_G = 260\,°C$ with the average CdSe coverage from 2.5–3.0 MLs. Fig. 2(e) clearly shows the ripened growth state for a CdSe coverage from 3.0–3.5 MLs, which is also schematically demonstrated in Fig. 4(d).

In addition to the above characterization by AFM, PL studies were also performed. The PL spectra for several samples with the CdSe coverage of 1.0 MLs–3.3 MLs were obtained at 10 K, as shown in Fig. 5(a). The peak position

clearly shifts toward lower energy as the CdSe coverage increases. Fig. 5(b) presents the dependence of the PL peak position on the CdSe coverage. Two linear dependences were found. The abrupt change in the slope was about 2.5 MLs, which its value is consistent with the critical thickness of the CdSe QD confirmed by AFM. The abrupt change in the slope could be correlated with the coherent SK QD structure formation. Restated, when the CdSe coverage is less than 2.5 MLs, the dependence of PL peak position with CdSe coverage exhibits a red shift and follows a linear behavior due to the size increase of the 2D-like islands as the CdSe coverage increases. When the CdSe coverage exceeded 2.5 MLs, the QD structure formed. It could be supposed that the 3D QD state has lower energy and stronger confinement, most of the excitons localized in the QDs to recombination. This emission dominates the PL spectra. As the CdSe coverage increased to 3.0 MLs, the broad PL line width contains the emission energies of the sample with 2.7 and 3.3 MLs. The significant broad band emission probably due to the recombination originated from excitons localized in complex states, for example, the 2D-like island, SK dot, and ripened dot. However, in the sample of 3.3 MLs, the narrow band width suggests a uniform dot distribution, in concert with AFM image. In summary, a complete transfer of the QD growth mode from the SK mode to the R_2 mode was observed in this report.

An in-chamber thermal annealing process was performed after the growth of CdSe QDs to control the dot size. Thermal annealing process at an appropriate T_A was expected to make the distribution of sizes uniform. Fig. 6(a) and (b) show the AFM plane view of samples 10 (the as-grown sample) and 11 ($T_A = 400\,°C$). In Fig. 6(a), two types of QDs, smaller QDs and larger QDs, were observed in sample 10. This sample is without thermal annealing. The dot density for both groups is approximately $6.7 \times 10^8\,cm^{-2}$. When $T_A = 400\,°C$, the dot density increased to $1.6 \times 10^9\,cm^{-2}$, and the dots had a uniform size. In Fig. 6(c), the dot size distributions (the number of dots versus the dot volume) of sample 10 and 11 were represented as open triangles and open squares, respectively. Solid and dotted lines are guides to the viewer. The dot volume was calculated based on the assumption that the dots are conical. The dot size distribution for sample 11 has only one peak, which is narrower than that for sample 10. The thermal annealing process at $400\,°C$ is determined to improve the size homogeneity of the QDs ensemble. Thus, the thermal annealing process may be a good artificial control to improve the fabrication of opto-electronic devices with QDs.

4. Conclusion

Self-assembled CdSe QDs were grown on the ZnSe buffer layer. The optimum growth temperature was found to be $260\,°C$. The coherent QDs observed from 2.5 MLs. Two types (SK mode and R_2 mode) of QDs were observed
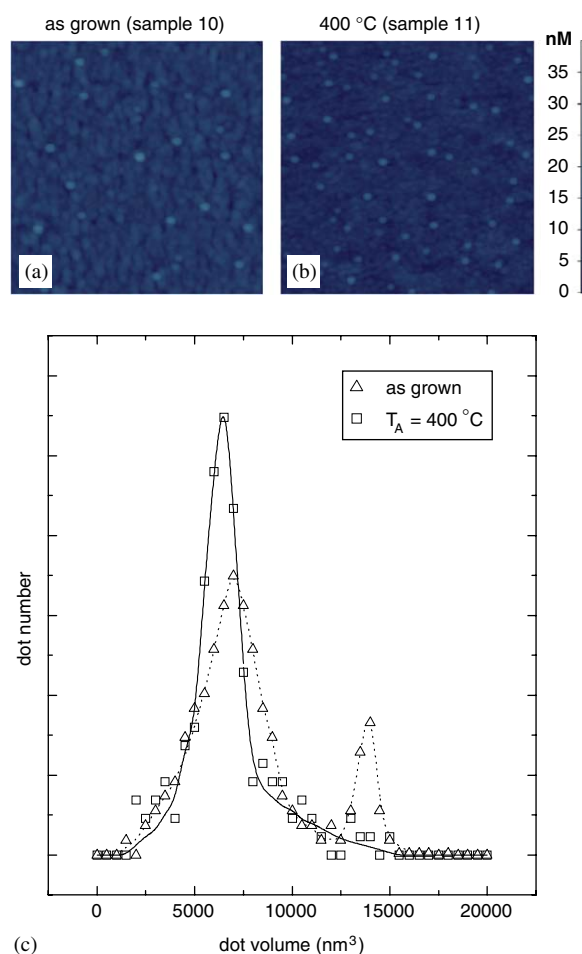

Fig. 6. (a) and (b) AFM images of samples 10 and 11. Thermal annealing process at $T_A = 400\,°C$ is used to control the dot size, and made the distribution of sizes uniform. (c) Dot size distributions (number of dots versus dot volume) of sample 10 (as-grown sample) and sample 11 ($T_A = 400\,°C$) are represented as open triangles and open squares, respectively. Solid and dotted lines guide the viewer. The dot volume was calculated by assuming the dots are conical.

when the average CdSe coverage was 3.0 MLs. A complete transfer of the QD growth mode from the SK mode to the R_2 mode was confirmed. A schematic diagram of growth dynamics of self-assembled CdSe QDs was presented. A dramatic change in the optical property verifies that the CdSe QDs formed about 2.5 MLs, which is consistent with the result of AFM studies. The post-growth control of the dot size distribution was achieved by the in-chamber thermal annealing. When the thermal annealing temperature was $400\,°C$, the dot size distribution was more uniform.

References

[1] J.C. Kim, H. Rho, L.M. Smith, H.E. Jackson, S. Lee, M. Dobrowolska, J.L. Merz, J.K. Furdyna, Appl. Phys. Lett. 73 (1998) 3399.

[2] L. Landin, M.S. Miller, M.-E. Pistol, C.E. Pryor, L. Samuelson, Science 280 (1998) 262.

[3] M. Bayer, O. Stern, P. Hawrylak, S. Fafard, A. Forchel, Nature (London) 405 (2000) 923.

[4] D. Bimberg, M. Grundmann, N.N. Ledentsov, Quantum Dot Heterostructures, Wiley, New York, 1998.

[5] K. Kitamura, H. Umeya, A. Jia, M. Shimotomai, Y. Kato, M. Kobayashi, A. Yoshikawa, K. Takahashi, J. Crystal Growth 214/215 (2000) 680.

[6] N.N. Ledentsov, I.L. Krestnikov, M.V. Maximov, S.V. Ivanov, S.L. Sorokin, P.S. Kop'ev, Zh.I. Alferov, D. Bimberg, C.M. Sotomayor Torres, Appl. Phys. Lett. 69 (1996) 1343.

[7] Y. Yang, D.Z. Shen, J.Y. Zhang, X.W. Fan, Z.H. Zhen, X.W. Zhao, D.X. Zhao, Y.N. Liu, J. Crystal Growth 225 (2001) 431.

[8] J.G. Belk, J.L. Sudijono, X.M. Zhang, J.H. Neave, T.S. Jones, B.A. Joyce, Phys. Rev. Lett. 78 (1997) 475.

[9] L. Goldstein, F. Glas, J.Y. Marzin, M.N. Charasse, G. Le Roux, Appl. Phys. Lett. 47 (1985) 1099.

[10] C.S. Kim, M. Kim, J.K. Furdyna, M. Dobrowolska, S. Lee, H. Rho, L.M. Smith, H.E. Jackson, E.M. James, Y. Xin, N.D. Browning, Phys. Rev. Lett. 85 (2000) 1124.

[11] H. Kirmse, R. Schneider, M. Rabe, W. Neumann, F. Henneberger, Appl. Phys. Lett. 72 (1998) 1329.

[12] S. Lee, I. Daruka, C.S. Kim, A.L. Barabási, J.L. Merz, J.K. Furdyna, Phys. Rev. Lett. 81 (1998) 3479.

[13] M. Rabe, M. Lowisch, F. Henneberger, J. Crystal Growth 184/185 (1998) 248.

[14] S.V. Ivanov, A.A. Toropov, S.V. Sorokin, T.V. Shubina, I.V. Sedova, A.A. Sitnikova, P.S. Kop'ev, Zh.I. Alferov, Appl. Phys. Lett. 74 (1999) 498.

[15] N. Matsumura, T. Saito, J. Saraie, J. Crystal Growth 227/228 (2001) 1121.

[16] S.H. Xin, P.D. Wang, A. Yin, C. Kim, M. Dobrowolska, J.L. Merz, J.K. Furdyna, Appl. Phys. Lett. 69 (1996) 3884.

[17] S. Lee, I. Daruka, C.S. Kim, A.L. Barabási, J.L. Merz, J.K. Furdyna, Phys. Rev. Lett. 81 (1998) 3479.

[18] J.L. Merz, S. Lee, J.K. Furdyn, J. Crystal Growth 184/185 (1998) 228.

[19] I. Daruka, A.L. Barabasi, Phys. Rev. Lett. 79 (1997) 3708.

[20] A. Endoh, Y. Nakata, Y. Sugiyama, M. Takatsu, N. Yokoyama, Jpn. J. Appl. Phys. Part 1 38 (1999) 1085.

[21] K. Leonardi, H. Heinke, K. Ohkawa, D. Hommel, H. Selke, F. Gindele, U. Woggon, Appl. Phys. Lett. 71 (1997) 1510.

[22] M. Strassburg, et al., Appl. Phys. Lett. 76 (2000) 685.

[23] I. Daruka, A.L. Barabasi, Appl. Phys. Lett. 72 (1998) 2102.

[24] D. Schikora, S. Schwedhelm, D.J. As, K. Lischka, D. Litvinov, A. Rosenauer, D. Gerthsen, M. Strassburg, A. Hoffmann, D. Bimberg, Appl. Phys. Lett. 76 (2000) 418.